

Coulomb-Field induced Light Particle Emission during Scission

B.Lindl, A.Brucker and J.P.Wurm

Max-Planck-Institut für Kernphysik, Postfach 103980, D-6900 Heidelberg, FRG

Scission-related emission of light-particles has been studied in the fusion-fission reactions $200, 254 \text{ MeV } ^{37}\text{Cl} + ^{124}\text{Sn} \rightarrow ^{161}\text{Ho}^*(f)$ (A,B; $E_x=100, 140 \text{ MeV}$) and $318 \text{ MeV } ^{28}\text{Si} + ^{141}\text{Pr} \rightarrow ^{169}\text{Ta}^*(f)$ (C; $E_x=207 \text{ MeV}$)^{1,2}. Light-particle spectra measured in coincidence with fission fragments at 200 angles in and out of the reaction plane are dominated by sequential emission: (i) from the composite nuclei (CNE), prior to scission ($M_\alpha \times 100 \simeq 1.1, 8.7, 38$ for A,B,C) and (ii) from fully accelerated fragments (FE) ($M_\alpha \times 100 \simeq 0.5, 4.5, 8$). At forward angles pre-thermalization emission is observed ($M_\alpha \times 1000 \simeq 0.31, 11.7, 33$). While absent in the proton spectra, near-scission emission (NSE) is disclosed in the α spectra by marked deviations from sequential emission at intermediate energies: a surplus yield perpendicular to ($M_\alpha \times 1000 \simeq 0.8, 13, 17$) and a deficit in direction of the scission axes ($M_\alpha \times 1000 \simeq 0.14, 10, 16$) reminiscent of the signature of ternary fission. In the reaction plane, fig. 1 visualizes these findings in case of exp.C by the quantity $R = \frac{dM}{d\Omega}|_{exp} / \frac{dM}{d\Omega}|_{CNE,FE}$, which is the ratio of the measured differential multiplicity to that for sequential emission -calculated by a 3-source calculation- for α (a) and proton emission (b).

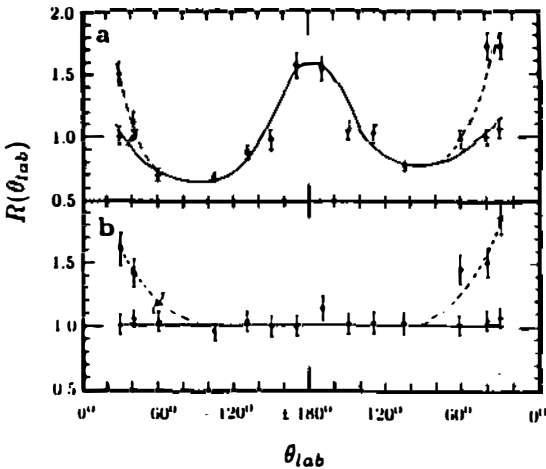
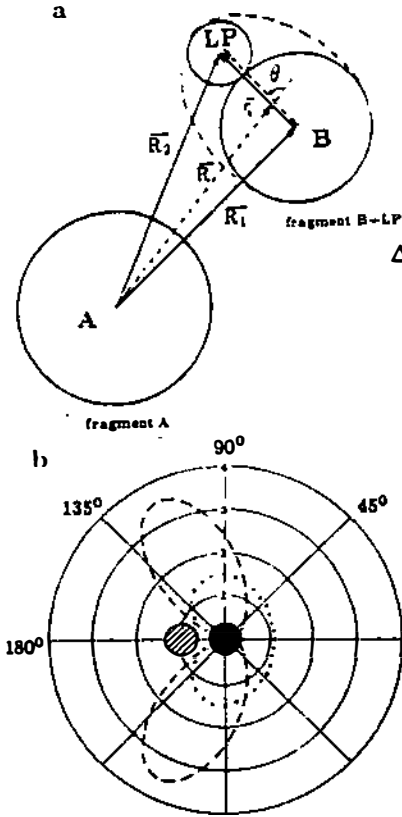


Fig. 1: Inplane angular distribution of $R(\theta)$ for α emission (a) and proton emission (b). $R=1$ means pure sequential emission, $R>1$ surplus and $R<1$ deficit yield. Prethermalization emission at forward angles is dashed.

From the out-of-plane measurements a doughnut-shaped spatial distribution of the α surplus yield around the cm scission axis is found and, by contrast, the deficit anomaly is disclosed to be marked as a cone in direction of the scission axis. By the observed scaling of the NSE-multiplicities vs. E_x with sequential multiplicities, NSE is identified as an evaporative process thus discarding the ternary fission picture.

As a new description we invoke Coulomb-field induced modulation of the evaporation barriers while fragments are in close contact, and within a simple static model we get reasonable agreement with the data. It is easily realized that the mutual

Coulomb field of adjacent fragments during or shortly after scission markedly influences the evaporation barrier and thus the intrinsic particle-emission probability. Fig. 2a depicts schematically light-particle (LP) emission at an angle θ with respect to the scission axis from the fragment B in the Coulomb field of fragment A.



The Coulomb barrier $V_{3B}(\theta, r_b)$ of the emitter in the 3-body configuration is given by the Coulomb barrier $V(r_b)$, describing the barrier without an adjacent fragment, and an additional angle-dependent modulation of the barrier $\Delta V(\theta, r_b)$: $V_{3B}(\theta, r_b) = V(r_b) + \Delta V(\theta, r_b)$, with

$$\Delta V(\theta) = \frac{Z_A Z_{LP} e^2}{R_2(\theta)} + \frac{Z_A Z_B e^2}{R_1(\theta)} - \frac{Z_A (Z_{LP} + Z_B) e^2}{R}$$

The additional term ΔV is simply the change of the Coulomb potential between B and LP due to the Coulomb potential of A at the barrier radius $r_b = |\vec{R}_2 - \vec{R}_1| = \text{const}$. According to the evaporation model³ this modulates the rate of emission $P \propto e^{-(B+V_b)/T}$ in the 2-body configuration by a factor $f(\theta) = e^{-\Delta V(\theta)/T}$.

Fig. 2: Schematic diagram of the scission configuration (a) where light-particle (LP) emission from fragment B+LP is considered in the close neighborhood of fragment A. Position vectors are indicated. (b) Polar diagram of the modulation factor $f(\theta)$ for α (dashed) and proton emission (dotted) from fragment B (solid circle) in the Coulomb field of fragment A (hatched). Static configuration, $R=11.5$ fm.

For symmetric fission of the composite nucleus ^{160}Ta (exp. C) we have calculated $f(\theta)$ (fig.2b) in various static configurations for proton (dotted) and α emission (dashed) as a function of the emission angle θ . In this configuration the Coulomb barrier for α emission is raised in direction of the scission axis ($\Delta V(\theta = 0^\circ) = +2.8$ MeV) and lowered perpendicular to the scission axis ($\Delta V(\theta = 90^\circ) = -2.4$ MeV). These calculations confirm the very different emission pattern of proton and α evaporation: the surplus and deficit in the α spectra correlated with the scission axis and the nearly absent anomaly for protons. For a more quantitative analysis including the dynamics and the time dependence of $f(\theta)$ we performed 3-body Coulomb-trajectory calculations including Coulomb-field emission during the scission process.

In conclusion we state that our data clearly exhibit a near-scission emission mechanism, and all the observed features of this emission process, including the scaling with excitation energy, are satisfactorily explained by our simple quasi-static model of Coulomb-field induced α emission from fragments during or shortly after scission, a process similar to Stark ionization in atomic physics.

1. A. Brucker et al., Phys. Lett. 186B (1987) 20
2. B. Lindl et al., submitted to Z. Physik A -Atomic nuclei-
3. H. Ho et al., Z. Physik A283 (1977) 235